The Journal of Experimental Biology 208, 4715-4725
Published by The Company of Biologists 2005
doi:10.1242/jeb.01950

In vivo mechanical properties of the human Achilles tendon during one-legged hopping

G. A. Lichtwark[1,*] and A. M. Wilson[1,2]

[1]*Structure and Motion Laboratory, Institute of Orthopaedics and Musculoskeletal Sciences, University College London, Royal National Orthopaedic Hospital, Brockley Hill, Stanmore, Middlesex, HA7 4LP, UK* and [2]*Structure and Motion Laboratory, The Royal Veterinary College, Hawkshead Lane, North Mymms, Hatfield, Herts, AL9 7TA, UK*

*Author for correspondence (e-mail: g.lichtwark@ucl.ac.uk)

Accepted 25 October 2005

Summary

Compliant tendons act as energy stores, which benefit the energetics and power output of a muscle–tendon unit. However the compliance of tendon and the material properties may vary between individuals and hence alter the energy storing capacity of the tendon. We aimed to determine the *in vivo* Achilles tendon (AT) stress and strain during one-legged hopping and hence the contribution of elastic recoil to mechanical energy changes. We simultaneously measured the length of the Achilles tendon from the muscle–tendon junction to the insertion on the calcaneous and the approximate AT force in ten male participants. The position of the muscle–tendon junction was determined using ultrasound images that were projected into three-dimensional space. Achilles tendon force was measured using inverse dynamics. The results demonstrated that one-legged hopping elicited high tendon strains and that the force–length relationship of the whole tendon is relatively linear, particularly at high strains. The stiffness, elastic modulus and hysteresis varied across the population (inter-quartile range of 145–231 N mm^{-1}, 0.67–1.07 GPa and 17–35%, respectively). These values are within the reported biological range. An average of 38 J of energy was recovered from the elastic recoil of the tendon, which contributes 16% of the total average mechanical work of the hop (254 J). The high strains measured here (average peak strain was 8.3%) and in other studies may be possible due to the complex architecture of the Achilles tendon; however, prolonged hopping may well cause tendon damage. In conclusion, the properties of the elastic Achilles tendon can contribute significantly to the total mechanical work of the body during one-legged hopping; however, individual variation in the properties of the tendon vary the energy storing capacity of this structure.

Supplementary material available online at
http://jeb.biologists.org/cgi/content/full/208/24/4715/DC1

Key words: elasticity, biomechanics, stress, strain, elastic modulus, human.

Introduction

Muscles attach to the skeleton *via* tendons, which transfer forces to the skeleton and the environment. Tendons consist primarily of a collagenous matrix that has elastic properties. This enables them to transmit force relative to the amount of the stretch that they experience (Koob and Summers, 2002). This mechanical property allows them to store and return elastic strain energy during locomotion and other movements (Roberts et al., 1997; Griffiths, 1991; Fukunaga et al., 2001; Alexander, 1988). In particular, the compliance of a tendon is critical in determining the time course of power output of the muscle (Roberts, 2002; Lichtwark and Wilson, 2005b). There have been few studies that have been able to directly determine tendon strain and energy storage in human tendons during real-life movements (Hof et al., 2002; Fukunaga et al., 2001). Here we apply a novel technique to determine the *in vivo* mechanical properties of the whole human Achilles tendon (AT) during a high strain movement.

The mechanical properties of tendon have been shown to be relatively uniform across a range of vertebrate animals (Bennett et al., 1986; Pollock and Shadwick, 1994). Many *ex vivo* mechanical tests have been carried out on tendon to determine how much energy it can store and return, its ultimate tensile strength and how repetitive loading affects the tensile strength (Bennett et al., 1986; Ker et al., 1986, 2000; Wang and Ker, 1995). However, much of this work has been carried out on cadaveric animal material, which may have undergone material changes as a result of the preservation process (Smith et al., 1996).

In vivo measurements of mechanical properties of the AT have demonstrated mixed results compared to those measured *ex vivo*. Measures of the mechanical properties of the AT have

demonstrated that there is variation in tendon stiffness and elastic modulus between individuals (De Zee and Voigt, 2001; Hof, 1998; Maganaris and Paul, 2002; Maganaris, 2002). Ultrasonography and magnetic resonance imaging (MRI) studies have recently reported strains of the AT ranging from 5–10% during isometric contractions at forces below the maximum possible force during dynamic movements (Finni et al., 2003; Muramatsu et al., 2001; Maganaris and Paul, 2002). It has previously been thought that such high strain would cause tendon rupture and failure; however real-life activities such as one-legged hopping can induce much larger stresses and strains on the AT without inducing acute rupture (Komi, 1990).

We seek to understand the amount of energy stored and returned from the AT under *in vivo* conditions where high strain is achieved. This will give an indication of the capacity for the AT to recycle mechanical energy during real-life movements and determine whether there is individual variation in the mechanical properties. We hypothesise that the AT acts like a classic energy storing spring, which stores and returns a substantial proportion of the energy required for the hopping movement. In addition, we hypothesise that the high strain movement will provide further evidence for variation in AT stiffness between individuals and more accurate measurements of tendon stiffness due to the greater range of strain data available.

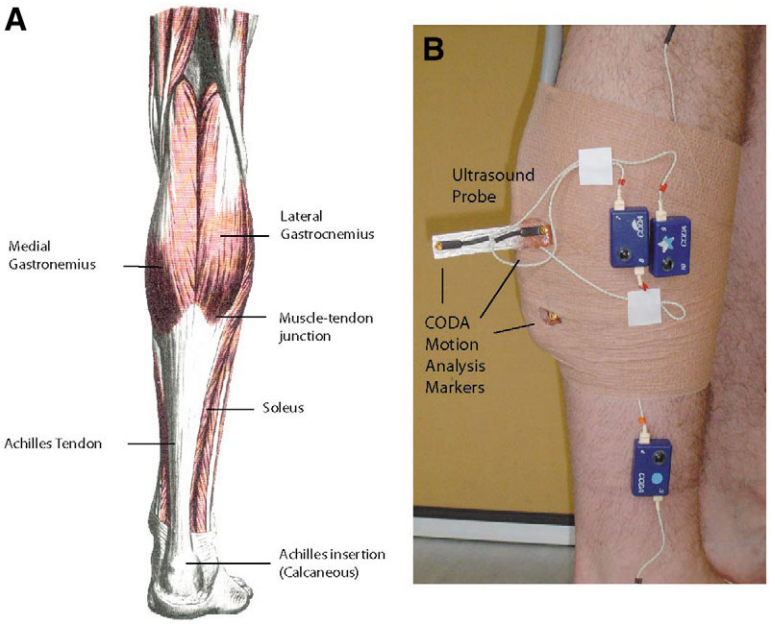

Fig. 1. (A) Anatomy of the triceps surae muscle group and the Achilles tendon (adapted from Gray's *Anatomy*). (B) Photograph of the attachment of the ultrasound probe to the leg. Three markers are rigidly attached to the probe by way of a fibreglass mould. This setup allowed for images of the gastrocnemius muscle–tendon junction to be visualised in the sagittal plane of the leg (see Fig. 2).

To test this hypothesis it is necessary to determine the length of the tendon and the force exerted during a dynamic activity that will induce large tendon strains. Therefore the aim of the experiment was to determine the *in vivo* AT length and force changes during one-legged hopping and hence the stress–strain relationships of individual ATs. We introduce a method that combines ultrasonography and motion analysis to make an estimate of the mechanical properties of tendons during the dynamic movement of one-legged hopping. This high force movement will allow a greater range of the force–length properties to be explored. Although it is likely that differential strain patterns will occur along the tendon (Finni et al., 2003; Lyman et al., 2004), in this paper we aim to determine the absolute force–length relationship during the high force activity of one-legged hopping. Unlike previously discussed ultrasound techniques for estimating tendon strain, this technique is the first that directly measures tendon length changes during dynamic movements and can potentially be applied to any movements, including locomotion.

Materials and methods

Achilles tendon strain and elongation

Strain is fractional elongation of the tendon. To determine this, the tendon length must be measured along with the length that corresponds to zero force. The AT length was defined as the distance between the tendon insertion and the muscle–tendon (MT) junction. To determine this length change, we used the CODA active marker, motion analysis system (Charnwood Dynamics, Leicestershire, UK) and determined the accuracy of length measurement in our experimental configuration to be better than 0.40 mm in 50% of cases. This is in line with the manufacturer's specification.

The AT runs from the insertion on the calcaneous to its junction with the triceps surae muscle group, which is most proximal at the junction with the two heads of the gastrocnemius muscle (Fig. 1A). The position of the insertion was tracked by attaching a CODA marker over the tendon insertion. In this position the light emitting diode (LED) attachment is within 4 mm of the tendon insertion and the offset is orthogonal to the tendon elongation. The effect of skin movement on tendon length was determined in the direction of action of the tendon using B-mode ultrasound imaging. This was done by placing an echogenic marker on the LED attachment site and taking sagittal plane images of the heel of the foot whilst it underwent the full range of motion used during one-legged hopping.

The position of the MT junction and the calcaneous relative to the global coordinate system was determined by a combination of ultrasonography and motion analysis. The MT junction was imaged by ultrasound whilst synchronously determining the position and orientation of the ultrasound image. Therefore the position of the MT junction could be

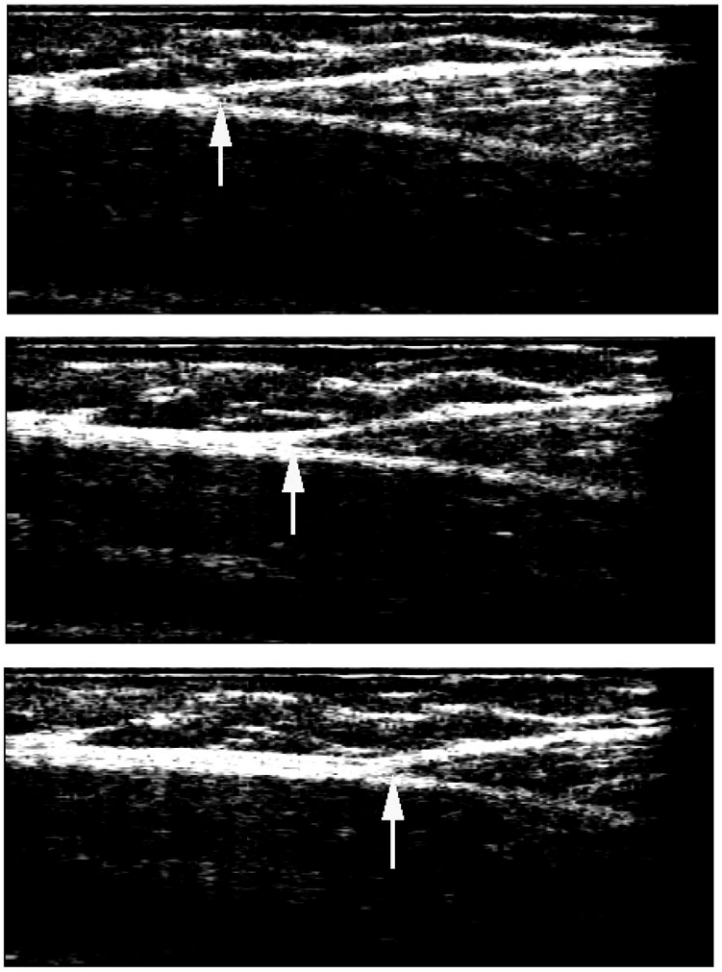

Fig. 2. Images of the Achilles tendon junction with the lateral gastrocnemius. The tendon is the thick white structure to the left of the arrow, while the muscle fascia branches off this white structure to the right. The arrows represent the point that was tracked in the image for each frame during the hopping movement. (See Video 1 in supplementary material).

projected into three-dimensional (3D) space and the distance from this point to the calcaneous marker determined as the AT length (Fig. 1B). Details of the methodology and potential sources of error of this method are discussed further below. Tendon strain at any time was determined by dividing the instantaneous length of the tendon by the length of the tendon at approximately 5% of the average maximum force achieved during the hopping movements (200 N). Due to the rapid rise in tendon force and the relatively low rate of strain measurement, as well as noise in the measurement, resolving the toe region in a single trial was not possible. Therefore when averaging trials, whilst a toe region would appear, this would be an artefact of the timing of individual points and the associated smoothing effect of averaging. We therefore preferred to cut off the data at 200 N, which would result in a slight underestimate of strain. The magnitude of this underestimate is difficult to quantify as published values vary, but it is likely to be less than 1%.

Determination of the muscle–tendon junction position

Movement of the MT junction site was determined by ultrasound imaging. A PC based ultrasound system (Echoblaster 128, UAB 'Telemed', Vilnius, Lithuania) was used to image the junction of the AT and the lateral gastrocnemius muscle fibres in the sagittal plane (Fig. 2). The junction was imaged approximately 1 cm lateral to the position where the medial and lateral gastrocnemius muscles join, which allowed for successful imaging of the MT junction. In this experiment we used a 128-element, linear, multi-frequency ultrasound probe at a frequency of 7 MHz and with a field of view of 60 mm in B-mode. Images were collected *via* USB link to a PC, recorded at 25 frames s^{-1} and saved as a video file for further analysis. The position of the MT junction was tracked in the two-dimensional (2D) image at each frame (Fig. 2).

Synchronous motion analysis allowed the position and orientation of the ultrasound probe in the global coordinate system to be determined. This was achieved by attaching three markers to the probe such that two markers lay along the axis of the ultrasound probe and one in approximately the same plane as the image, a distance of approximately 70 mm away from the line of the other two markers (Fig. 1). The motion analysis data were synchronised with the ultrasound data using a digital output signal from the CODA motion analysis system that signified that the system was collecting data. This signal activated a signal generator that fed a 5 MHz signal to a sonomicrometry crystal (Sonometrics Ltd, Ontario, Canada) attached to the end of the ultrasound probe. This produced a white signal on the edge of the ultrasound image that indicated that the CODA system was collecting data. The motion analysis data were collected at 100 Hz, therefore accuracy of the synchronisation was within 0.04 s.

The position of the ultrasound image relative to the probe coordinate system was required so measurements in the ultrasound image plane could be projected into the 3D global coordinate system. To do this, the point of a metallic wand was tracked in 3D space using three CODA markers attached to the wand. The position of the wand tip relative to the three markers was first determined and the tip of the wand was then immersed into a water bath that was scanned by the ultrasound probe. Because metal is highly echogenic, it was possible to easily identify the point of the wand when it was in the plane of the images being scanned by the ultrasound probe. Three points (relative to the probe axis frame) in the plane of the image are required to translate the 2D coordinate data back into the 3D space. The average coordinate of three corners of the image were chosen to define the image plane relative to the three markers defining the probe axis system.

Points tracked in the 2D ultrasound image could then be embedded back into the laboratory frame of reference to get the 3D position relative to the laboratory. This was a two-step procedure. First the coordinates measured in the 2D image were

embedded into the corresponding probe axis system, which was fixed relative to the image. The marked 3D coordinates were then embedded into the laboratory reference frame.

Ultrasound accuracy and sources of error

To determine the accuracy of the calibration and ultrasound measurements, we scanned a Perspex® phantom located in the laboratory coordinate system that consisted of two Perspex sheets with grooves cut into them, which corresponded to an approximate length and position of the muscle fibres relative to the skin (Fig. 3). The phantom was immersed in a plastic container full of water so that the phantom grooves could be scanned from the outside of the container in a direction equivalent to that in which the MT junction is imaged on the leg (the *x*–*z* plane of the laboratory coordinate system). The position of the bottom edge of each of the grooves relative to the laboratory was determined by running the point of the previously used metallic wand along the grooves and tracking these points. A 3D regression line was fitted through the data to represent the position of the grooves in the laboratory space. The phantom was then scanned with the ultrasound probe and the position of the image in the laboratory space was tracked synchronously using the previously mentioned methods. Visible points on the bottom edge of the grooves were marked in frames where the grooves were visible. These points were then embedded into the global coordinate space and a comparison between these points and the fitted regression line made.

To determine the effect of rotation of the probe on the length of the AT, the probe was manually rotated about the long axis of the leg and also around the medio-lateral axis of the leg. These rotations were chosen as they are likely to result in images of a different region of the MT junction and potentially cause measurement error. Rotation of the image plane was measured relative to a plane of the leg defined by the lateral malleolus, lateral head of the proximal fibula and lateral epicondyle of the femur.

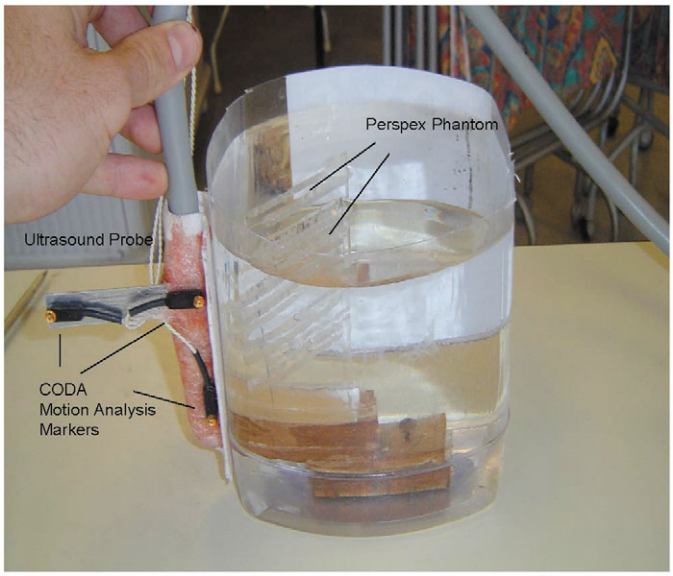

Fig. 3. Photograph of the Perspex phantom emerged in water and imaged by the ultrasound probe (with rigidly attached markers). The positions of the grooves relative to the laboratory were recorded by tracking the tip of a wand as it move along the grooves. The positions of the grooves were also determined with the ultrasound probe using the technique described and a comparison made between the two.

Achilles tendon force and stress

The 3D ground reaction force was measured using a Bertec force plate at 1000 Hz (Bertec Corporation, Columbus, OH, USA) and the motion analysis global coordinate system was aligned to the force plate so that the ground reaction vector could be transformed into it. The inertial properties of the foot segment as defined by Plagenhoef et al. (1983) were used in an inverse dynamics solution to calculate the ankle plantar flexor moment at the joint centre. This was defined as the moment about the axis perpendicular to the plane defined by the calcaneous marker, the ankle joint centre of rotation and the insertion of the AT.

The ankle joint centre was estimated by creating a virtual point corresponding to an approximation of the centre of rotation of the ankle. This point was half the distance between the lateral and medial malleoli, perpendicular to the plane created by markers placed on the fifth metatarsal, the calcaneous and the lateral malleolus. This effectively corresponds to a position midway between the lateral and medial malleoli.

AT force was calculated by dividing the ankle joint moment by the moment arm between the AT and the ankle joint centre. This was calculated at each time point as the perpendicular distance from the ankle joint centre to the line of action of the AT (the direct line from the calcaneous to the projected position of the muscle–tendon junction). It was assumed that all of the plantar flexor moment was contributed *via* the AT structure. Tendon stress was calculated for each individual by dividing the instantaneous force by the minimum cross sectional area (CSA) of the AT. CSA was measured by taking an ultrasound scan across the tendon in the coronal plane.

Participants

Ten male participants, average age 30.9 (±8.2) years, gave written consent to take part in the study, which was approved by a local ethics committee (RNOH JREC, 04/Q0506/11). The participants were asked to step onto the force plate and hop continuously on one leg on the spot at a frequency of approximately 2 Hz (average contact time=0.32 s). An average of 45 hops were performed across three bouts with rest breaks between every 15–20 hops. Simultaneous force plate, 3D motion analysis and ultrasound data were collected and synchronised during the hopping periods as previously described. One participant performed the experiment on 3 separate days so that the repeatability of the measures could be determined.

Marker positions and measurements

The instrumented ultrasound probe was attached to the leg with Coban™ tape (3M, St Paul, MN, USA) such that the lateral gastrocnemius muscle–tendon junction could be imaged. Further active markers were placed on the following

anatomical landmarks: head of the fifth metatarsal, proximal calcaneus (at the approximate insertion site of the AT), lateral malleolus, head of the fibula, lateral femoral epicondyle and on the ilotibial band (halfway between the greater trochanter and the lateral epicondyle).

Ankle and knee joint angles were calculated in two dimensions (in the plane of the hopping movement) using the markers previously mentioned. Total gastrocnemius muscle–tendon unit (MTU) length was estimated from these angles by applying the equations of Grieve et al. (1978). The length change of the muscle belly (including other series elastic structures like aponeurosis) was calculated by subtracting the measured AT length change from the MTU length change.

Data analysis

Individual subject data were used to create an average force–length and stress–strain relationship. This was done by filtering the length data with a fourth order, 5 Hz low-pass Butterworth filter and time interpolating the force and length measurements to 50 points across the period of foot contact (when the ground reaction force was above 0 N) on each hop. The ground reaction force during hopping was symmetrical in time (i.e. the time course of force rise was similar to the time course of force fall), and therefore this method of interpolation means that the peak force (and strain) will occur at very similar times within the hop. The time point where the AT force was 200 N was taken as the time point of zero length (or slack length) of the tendon to maintain a consistent measure of tendon length under small loads (5% of the total average tendon force during the hop). Tendon stiffness (slope of the force–length curve) and the elastic modulus (slope of the stress–strain curve) of the tendon were determined by placing a linear regression through the averaged force–length data for each individual. Hysteresis was calculated by dividing the difference between the area under the loading and the unloading curves by the area under the loading curve alone. This provides a measure of the energy converted to heat, an important feature of the mechanical properties of tendon (Wilson and Goodship, 1994).

To determine the amount of energy contributed to work of the hop, the energy recovered from the tendon was determined as the area under the descending limb of the force–length curve. The amount of work associated with each hop was determined as the maximum potential energy for the hop relative to the lowest point. This was calculated using the vertical ground reaction force measured with the forceplate using methods described in Cavagna (1979). The relative contribution of the AT recoil to the work of the hop was determined by dividing energy recovered from the tendon by the total work of the hop. This was averaged across all hops for each participant and a population average was determined from this.

Results

Ultrasound accuracy and sources of error

The effect of skin movement on the predicted site of the insertion of the AT was found. The amplitude of the distance between the tendon insertion and the skin marker was measured in the direction of the tendon, and average amplitude of skin movement across the range of movement was 1.9 mm. This corresponds to an approximate maximum strain error of 0.79% across the range of the movement.

A scan of the Perspex® phantom with the ultrasound-motion analysis setup allowed for comparison between the predicted position of the grooves of the phantom and regression lines fit to the position of these grooves (as measured by motion analysis) to be made. A 3D reconstruction of the points measured with both techniques can be seen in Fig. 4A, while a comparison in 2D for each Perspex® sheet (in the plane of the sheet) is shown in Fig. 4B. In 3D the error was less than 1.15 mm for 50% of the observations (Fig. 4C); however, much of this error is in the laboratory x–y plane. In the x–z plane, which is the plane where much of the length change in the AT length was measured, the accuracy was within 0.96 mm for 50% of the cases (Fig. 4C).

Measurement of the AT length during manual rotation of the ultrasound probe resulted in a maximum error of 2.6 mm within the range of rotation recorded during the hopping activity (average range 22.9° in the long axis and 0.8° in medio-lateral axis). This corresponds to an approximate maximum error in our strain measurement of 1.08%. However, most of the rotation occurs during the initial loading and final unloading of the tendon, which will affect the stiffness at these times only.

Achilles stiffness and force–length properties

An example of the relationship between the instantaneous measurements of AT force and AT length for an individual during the periods of foot contact is shown in Fig. 5. The effect of filtering the AT length is also demonstrated. There is a clear relationship between the measured length and force, where an increase in force corresponds to a relatively linear increase in tendon length. On initial increase of AT force, the length increases at a higher rate than when the tendon is almost fully loaded (at the highest forces) and generally displays patterns of hysteresis, where the Achilles force is less for any given length during unloading compared to loading. The force and length both rise and fall in a sinusoidal fashion, which is typical of a one-dimensional spring mass system.

The average gastrocnemius MTU length change and the AT length change for the population are shown in Fig. 6. This comparison reveals that the AT does not stretch as much as the whole MTU. It does, however, account for over 80% of the length change throughout the majority of the hopping cycle. Further length change must occur in the muscle belly, either in the muscle fibres or in the aponeurosis and proximal tendon insertions of the gastrocnemius muscles.

The average force–length relationship for one individual participant on 3 separate days is shown in Fig. 7. The change in length is measured from the zero force length and all three trials correspond closely, with AT stiffness being 188, 187 and 170 N mm^{-1} on each measurement occasion.

The force–length relationships for all ten subjects and the starting length adjusted force–length relationships are shown in

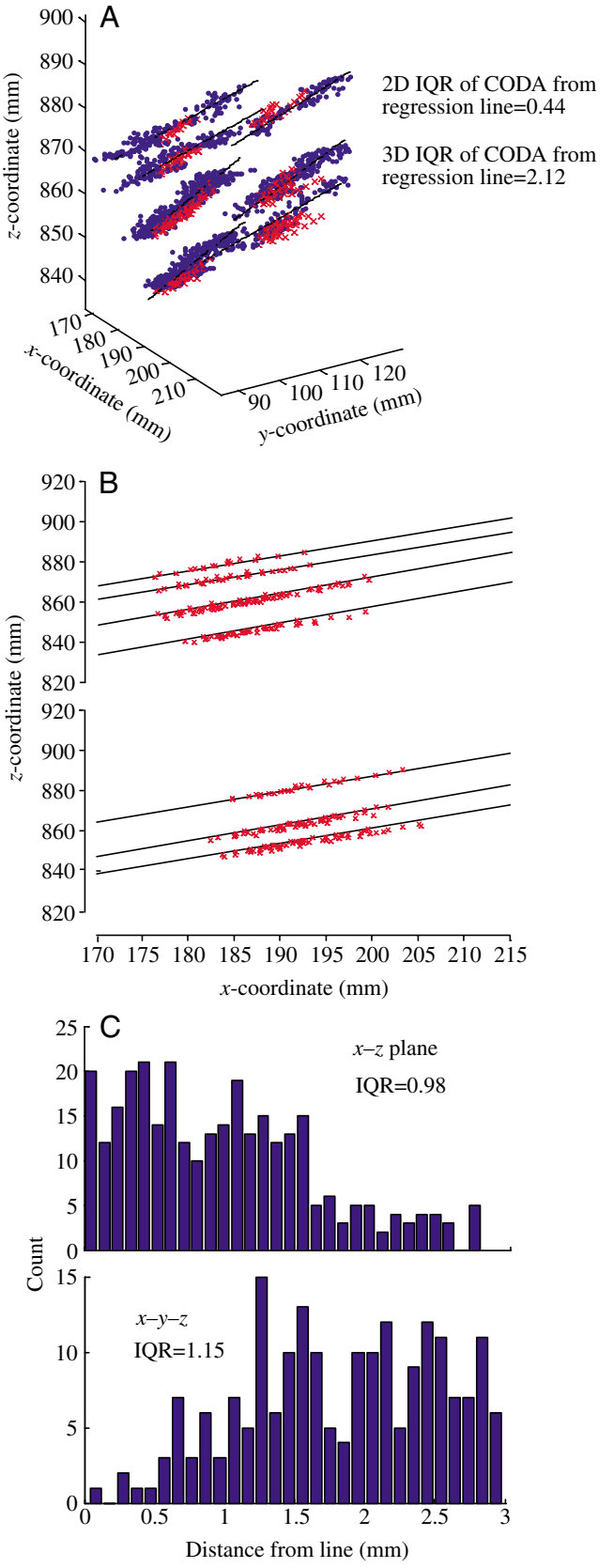

Fig. 4. (A) Three-dimensional (3D) reconstruction of the position of the Perspex® grooves of the phantom by tracking the tip of a wand with motion analysis (blue) and embedding the position of the grooves when visualised by an ultrasound probe into the laboratory frame of reference (red). The line represents a 3D regression line placed through the motion analysis data for each groove. The inter-quartile range (IQR) of the perpendicular distance of the motion analysis measured coordinates along the Perspex® grooves from the regression line in both 2D (*x*–*z* plane) and the 3D were 0.44 mm and 2.12 mm, respectively. (B) Two-dimensional (2D) comparison of the position of the grooves as determined by regression through the motion analysis data and the position determined by the ultrasound technique for each Perspex® plate. This was measured in the same plane (*x*–*z*) that was used to image the muscle–tendon junction during the hopping experiments. (C) Histogram of the error of the ultrasound technique compared to the calculated regression line that represents the position of the phantom grooves in both 2D and 3D. The IQR of the perpendicular distance from the measured coordinates of the grooves measured with the ultrasound technique to the linear regression line in both 2D (*x*–*z* plane) and 3D were 0.98 mm and 1.15 mm, respectively.

Fig. 8A,B respectively. There is a broad range of zero lengths for the AT across the small subject group, and the stiffness of the ATs (slope of the lines shown in Fig. 8) is also variable between individuals. Generally the results suggest that the tendons don't display the classical toe region where the stiffness of the tendon should be lower during the initial loading. Instead the opposite is true for the majority of participants, with an initially higher stiffness at low loads during loading. However, during unloading the stiffness is generally lower at smaller loads.

Achilles material properties and contribution to work

The stress–strain relationships for three individuals representing the whole range of elastic moduli across the group is demonstrated in Fig. 9A. A linear regression was performed through each subject's average data and the elastic modulus recorded as the slope of this line. Due to interpolation with respect to the time for each individual hop and the sinusoidal loading pattern, more of the points acquired in each individual hop were recorded at high loads and strains. An average stress–strain relationship for all participants is demonstrated in Fig. 9B. This figure also shows the standard deviation in both stress and strain measures during the hopping movements. The greatest deviation in strain measurement is apparent at lower stress values. An average hysteresis of 26% was recorded across all subjects, but these values varied greatly with the inter-quartile range being 17–35%.

The average material and architectural properties of each individual's tendon, including stiffness, CSA, elastic modulus and apparent hysteresis are shown in Table 1, which also presents the average energetics associated with the hopping movement for each individual. These results show that there is indeed a range of AT stiffness across the population and this is also reflected in calculated elastic modulus. Similarly there is a range of hysteresis measured, with a mean of 26%. Both the energy recovered from the tendons and total mechanical work varied from subject to subject, and thus an inter-quartile range of 10–21% of the total mechanical work was found to be contributed to by the energy recovery from the AT. Peak

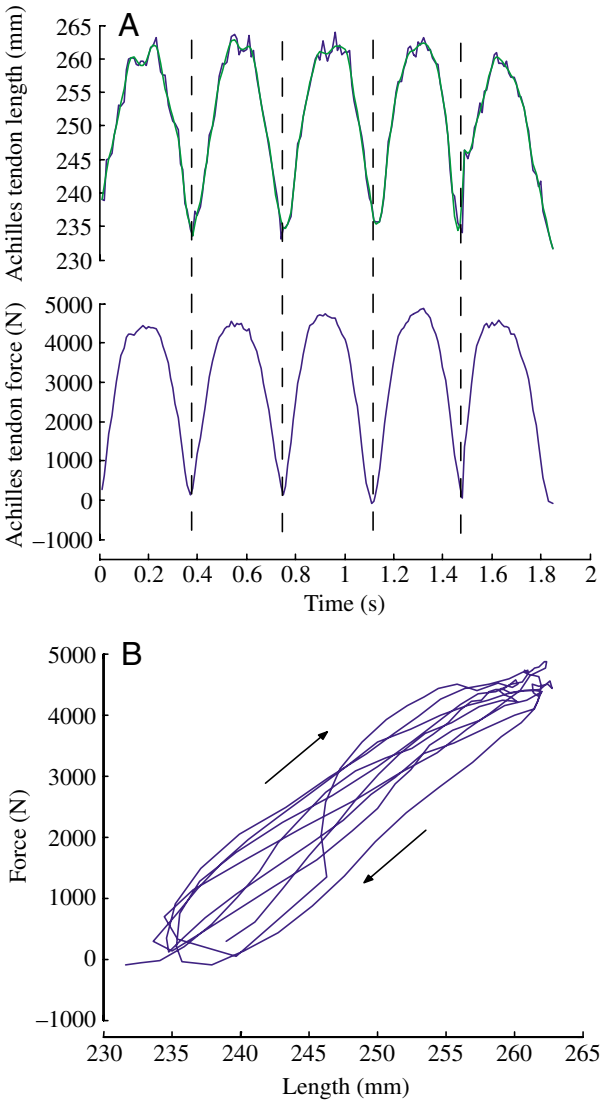

Fig. 5. (A) Achilles tendon (AT) length and force measurements against time for five consecutive hops. AT length is shown in the raw form (blue) and after applying a fourth order, 5 Hz low-pass Butterworth filter (green). Note that only periods of contact have been displayed and subsequent data during time off the ground were removed. (B) Force against length for the same five trials as in A. Arrows represent the general trend for rise and fall of the force against length. (For an animation of stick figure, see Video 2 in supplementary material)

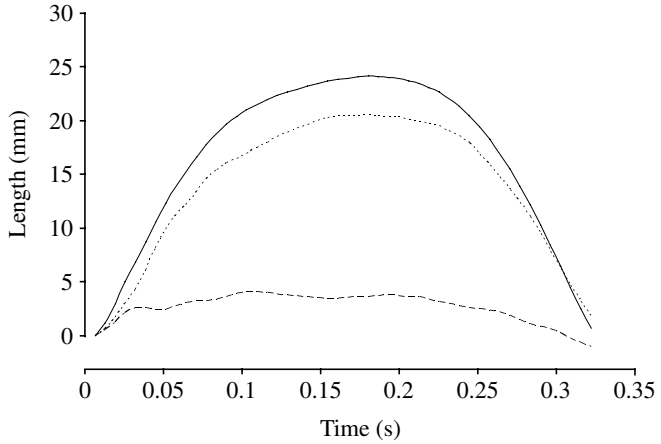

Fig. 6. Average change in Achilles tendon length (dotted line), gastrocnemius muscle–tendon length (solid line) and approximate muscle length (broken line) during a single hop. The muscle length represents both the length of the fibres and the also other serial elastic tissues including the proximal tendon and aponeurosis.

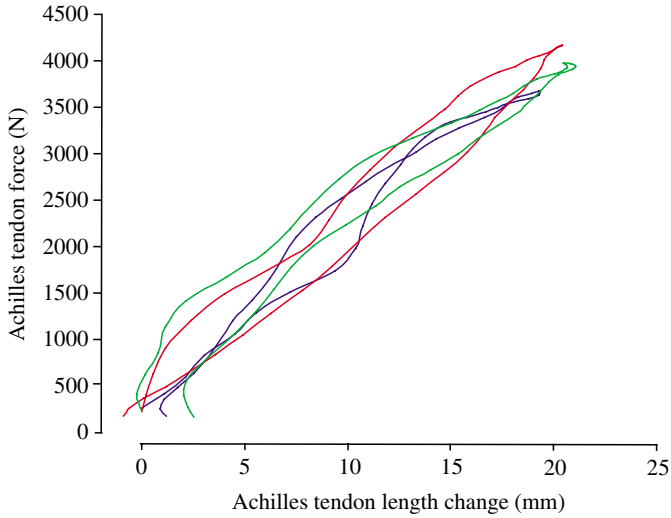

Fig. 7. Average Achilles–tendon force *vs* the change in Achilles tendon length (relative to the length at 200 N) for the same subject over three separate measurement occasions (blue, trial 1; green, trial 2; red, trial 3).

tendon strain was also variable between subjects with a range of 6.2–10.3% strain. Although it is reasonable to suggest that a relationship between body mass and/or activity and tendon stiffness or cross-sectional area may exist, the small range of body masses in our group precludes attaining useful correlations between these variables.

Discussion

In the present study we have used a novel technique that has allowed measurement of tendon strain during very high strain movements. Large whole tendon strains were achievable during one-legged hopping. There was individual variation in the material properties of the AT across the group of participants assessed here, though the material properties were within the previously published range. The results indicated that the AT does indeed act like an energy storing spring by contributing a considerable amount of energy to the total mechanical work performed.

Achilles tendon as an energy saving mechanism

Combining traditional motion analysis with ultrasound imaging to determine whole tendon length changes during dynamic activities provides an ideal technique to study

muscle–tendon unit interaction. The results of this study demonstrated the energy storing capabilities of the AT, whereby the tendon stretches in proportion to the force applied during the downward motion of the body and then recoils to release most of the energy stored (74%) during the upward movement. This provides a substantial amount of the total mechanical energy of the hop (16%). This mechanism has been thought to provide an energy saving mechanism during human walking, running and jumping (Alexander, 1988; Bobbert et al., 1986; Fukunaga et al., 2001) and has recently been suggested to account for up to 6% of the total mechanical work produced during walking (Maganaris and Paul, 2002). This research therefore further shows the capacity of the body to utilise elastic stain energy and provides a valuable technique for quantifying tendon strain and energy storage capacity in further real-life movements such as walking and running. However, application of this technique in lower force activities may result in broader measures of strain due to the larger variation in strain measured at the low forces in this study.

Most of the length change occurring in the MTU occurs in the AT (Fig. 6), thereby the return of elastic energy during tendon recoil provides most of the shortening work required for take-off. In contrast, the muscle (plus other series elastic structures such as the proximal tendon and aponeurosis) only stretch and shorten by small amounts during the hop, thereby reducing the work required by the muscle fibres. This is energetically efficient because it requires less work by the muscle fibres and reduces the heat produced from actively shortening the muscle fibres (Lichtwark and Wilson, 2005a). The aponeurosis associated with the medial gastrocnemius has also been found to be highly compliant and therefore some of the stretch and recoil occurring in the muscle fibres/aponeurosis complex may be elastic strain energy as well. This would allow the muscle fibres to act almost isometrically, which has been suggested to be the most efficient manner to operate (Roberts, 2002).

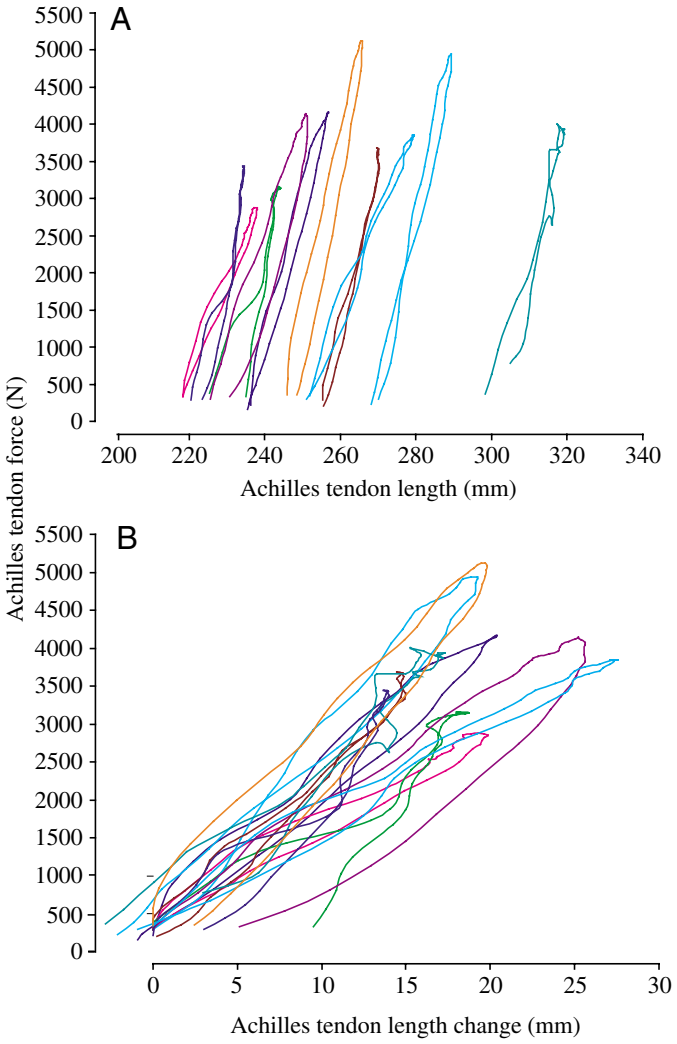

Fig. 8. (A) Average Achilles tendon force–length relationship for 10 individual participants. (B) Average Achilles tendon force *vs* change in length (relative to the length at 200 N) for each of the 10 participants.

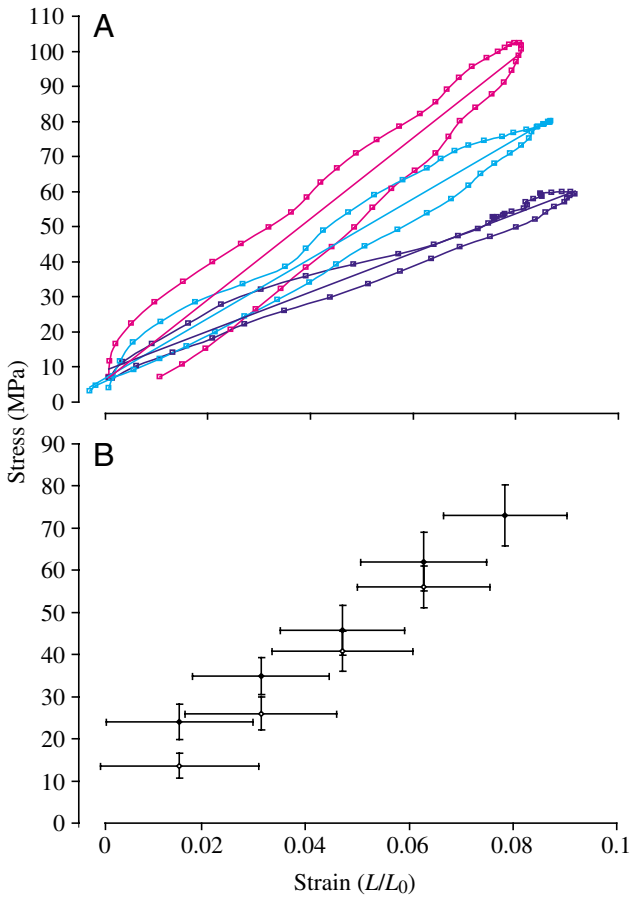

Fig. 9. (A) The average stress–strain relationship for three participants across the range of elastic moduli determined. The elastic modulus for each individual was determined by fitting a linear regression through the stress–strain data, as displayed. (B) Group average stress–strain relationship at five points during both loading (filled diamonds) and unloading (unfilled diamonds) during the hopping movement and the standard deviation of stress and strain measurements (error bars indicate ±1 S.D.).

Achilles tendon material properties and strain

The strains measured here are at the higher end of those expected before tendon rupture, based on *ex vivo* material testing. Typical tensile testing of tendinous material suggests that it should begin to fail at strains from 6–10% (Bennett et al., 1986; Ker et al., 1986); however, here we have measured whole tendon strains of over 10% without failure or injury. One-legged hopping was chosen specifically because it is an activity that should elicit very high stress and strain in the tendon. There are also major differences in what is actually measured between other techniques. For instance, most *ex vivo* tensile testing is performed on sections of tendon, typically where the cross-sectional area is least. In contrast, here we have made a measure of whole tendon length. It is well documented that large strains can occur in tendinous material with some estimates of aponeurosis strain during contraction being as high as 50% (Zuurbier et al., 1994). Therefore whole tendon strain is likely to differ from material testing results for samples of tendon.

Nonetheless, the force–length and stress–strain properties of the AT measured are within estimates of animal tendon (elastic modulus, 0.4–1.7 Gpa; Zajac, 1989) and also *in vivo* measurements on the AT (stiffness, 150 N mm^{-1}; elastic modulus, 1.16 Gpa; Maganaris and Paul, 2002). In addition, we have measured hysteresis values within the normal range (3–38%). The average value of 26% is similar to that recently found to occur in the tibialis anterior and gastrocnemius tendons (19 and 18%, respectively; Maganaris and Paul, 2002; Maganaris, 2002). The lack of a toe-region in our stress–strain data may be the result of low accuracies at low forces, or because we used a value of 200 N of tendon force as the cut-off to estimate zero strain. Taking a zero of 200 N will result in a small (less than 1%) underestimate of actual strain.

There are also measurement reasons why such high strains might have been measured. Firstly, it is likely that the measurement technique introduced some systematic errors in the calculation of the tendon length. The typical rotation of the probe around the tendon (hence changing the region of the muscle–tendon junction tracked) has been shown to overestimate the Achilles strain by approximately 1.08%. Because this rotation occurs mainly during impact and take-off of the hop, then the estimate of slack length of the tendon may be incorrect (but not tendon stiffness). This may be responsible for the lack of toe-region in the force–length data for most subjects during the initial loading of the tendon. In addition, the muscle contraction under the skin may distort the junction and alter the results during muscle shortening on impact with the ground.

It is also possible that the 3D structure of the AT allows high strains to be achieved. The structure of the AT varies dramatically along its length, from a uniform, round, cross-sectional area distally to a fan shape more proximally (Fig. 1). It is possible that shape changes of the fan region of the tendon and the muscle may help to achieve such high strains. This could be further explored by making ultrasound measurements of tendon shape change during the movement. This could be achieved with consecutive scans of the tendon at different positions on the muscle–tendon junction and in different planes, or perhaps by applying new four-dimensional ultrasound techniques that can image volumes of tissue in time.

Numerous other studies have suggested that high levels of strain occur in the AT and also other elastic structures. Recent ultrasonography studies during isometric and dynamic movements have reported that strains of the series elastic element (both the tendon and aponeurosis) can exceed 10% (Kubo et al., 2002). These studies do not, however, distinguish between distal tendon, proximal tendon or aponeurosis. A more direct ultrasound study also achieved strains of 5% (12 mm) during an isometric contraction (Maganaris and Paul, 2002); however, these contractions could only achieve small forces

Table 1. *Average mechanical and architectural properties of the Achilles tendon for each participant and the average energy recovered from the tendon and its contribution to the total average work performed on the body for each participant*

Subject no.	Mass (kg)	CSA (mm^2)	Stiffness (N mm^{-1})	Elastic modulus (GPa)	Peak strain (%)	Hysteresis (%)	AT energy recovered (J)	Total mechanical work (J)	% AT contribution
1	92	59	205	0.90	4.3	20	21	170	8
2	81	52	187	0.85	8.6	17	40	237	17
3	67	49	122	0.61	9.1	24	33	191	20
4	73	56	175	0.71	8.3	38	29	451	10
5	94	56	229	1.11	7.1	15	48	244	18
6	87	48	153	0.72	11.4	39	34	275	14
7	97	56	230	0.94	4.7	33	52	296	12
8	69	54	234	0.63	6.3	19	19	166	10
9	69	53	223	1.07	8.0	21	57	233	24
10	81	50	125	1.15	10.9	35	41	275	24
Average	81	53	188	0.87	8.3	26	38	254	16
S.D.	11.2	3.6	43.2	0.2	2.1	9.2	12.6	82.3	5.9

The population average and standard deviations (S.D.) are shown.
For abbreviations, see list.

compared to those obtained here during one-legged hopping. Using phase-contrast magnetic resonance imaging, strains of approximately 4.7% were achieved during a 40% maximum isometric contraction (Finni et al., 2003), therefore it does seem that the AT can achieve large levels of strain, at least for a limited number of cycles, without rupture. Taking these results into account as well as the strain records measured here, it is apparent that high AT strains are indeed achieved during human movement. The hopping movement is a particularly high force movement and therefore should elicit extreme strains, and prolonged one-legged hopping, which rarely occurs in everyday activities, may well begin to damage the AT.

Individual variation

The individual tendon stiffness and elastic modulus show a relatively broad range across the subject group measured. Although broad studies of different animals suggests that there is little variation in the elastic modulus, there is some evidence that this can vary with training effects (Buchanan and Marsh, 2001; Reeves et al., 2003). Therefore, with such a small group, the variation may be exaggerated. In addition, while the technique seems to be reproducible for one participant (Fig. 7), there is still room for individual variability that is inherent to the technique. For instance, the protocol does not control for individual muscle architecture and also muscle activation during the movement. Individual muscle architecture could influence the force–length relationship due to differences in probe rotation (as previously mentioned) and also the shape of the tendon insertion relative to the orientation of the probe (and hence image plane). Muscle activation has also been suggested to influence the stiffness of the series elastic structures (Hof, 1998, 2003), and not controlling for this may influence the AT stiffness in some way. Finally the contribution of the soleus and lateral gastrocnemius to the force that strains the AT may differ between participants and effect the measured whole tendon length change.

Conclusions

In conclusion, the current study has provided a new technique for the measurement of whole tendon length during dynamic activities. We have measured the length of the AT from the muscle–tendon junction to its insertion to the calcaneous using a combination of motion analysis and ultrasound. During the high strain movement of one-legged hopping, the elastic behaviour of the AT is highlighted, where a substantial amount of the mechanical energy required to produce the hopping movement is provided by elastic recoil of the AT. The majority of the strain occurs in the AT compared to the muscle contractile component and aponeurosis and this allows for rapid recoil of the muscle–tendon unit during take-off. Synchronous measurement of AT force has shown that typically linear force–length properties of tendons under high forces can be reproduced. The mechanical properties of the tendon are within the measured physiological range, despite high measures of whole tendon strain that result from the high forces. These high strains may be the result of the complex 3D fan shape of the AT, which may allow for such high whole tendon strains in the direction of muscle action due to shape change.

List of abbreviations

AT	Achilles tendon
CSA	cross-sectional area
IQR	inter-quartile range
LED	light emitting diode
MRI	magnetic resonance imaging
MT	muscle–tendon
MTU	muscle–tendon unit
3D	three dimensional
2D	two dimensional

The authors would like to acknowledge their funding bodies. G.L. receives financial support from the British Council Overseas Research Fellowship and the Royal National Orthopaedic Hospital Trust Research and Development Scholarship. A.W. receives support as a BBSRC Research Fellow and holder of a Royal Society Wolfson Research Merit award. The authors would also like to acknowledge Dr Renate Weller (Royal Veterinary College, UK) and Prof. Roger Woledge (Kings College London, UK) for their technical help and advice.

References

Alexander, R. M. (1988). *Elastic Mechanisms in Animal Movement*. Cambridge: Cambridge University Press.

Bennett, M. B., Ker, R. F., Dimery, N. J. and Alexander, R. M. (1986). Mechanical properties of various mammalian tendons. *J. Zool. Lond.* **209**, 537-548.

Bobbert, M. F., Huijing, P. A. and Ingen Schenau, G. J. (1986). An estimation of power output and work done by the human triceps surae muscle-tendon complex in jumping. *J. Biomech.* **19**, 899-906.

Buchanan, C. I. and Marsh, R. L. (2001). Effects of long-term exercise on the biomechanical properties of the Achilles tendon of guinea fowl. *J. Appl. Physiol.* **90**, 164-171.

Cavagna, G. A. (1979). Force platforms as ergometers. *J. Appl. Physiol.* **39**, 174-179.

De Zee, M. and Voigt, M. (2001). Moment dependency of the series elastic stiffness in the human plantar flexors measured in vivo. *J. Biomech.* **34**, 1399-1406.

Finni, T., Hodgson, J. A., Lai, A. M., Edgerton, V. R. and Sinha, S. (2003). Nonuniform strain of human soleus aponeurosis-tendon complex during submaximal voluntary contractions in vivo. *J. Appl. Physiol.* **95**, 829-837.

Fukunaga, T., Kubo, K., Kawakami, Y., Fukashiro, S., Kanehisa, H. and Maganaris, C. N. (2001). In vivo behaviour of human muscle tendon during walking. *Proc. R. Soc. Lond. B* **268**, 229-233.

Grieve, D. W., Pheasant, S. and Cavanagh, P. R. (1978). Prediction of gastrocnemius length from knee and ankle joint posture. In *Biomechanics*, Vol. VI-A (ed. E. Asmussen and K. Jorgensen), pp. 405-412. Baltimore: University Park Press. **2**, 405-412.

Griffiths, R. I. (1991). Shortening of muscle fibres during stretch of the active cat medial gastrocnemius muscle: the role of tendon compliance. *J. Physiol.* **436**, 219-236.

Hof, A. L. (1998). In vivo measurement of the series elasticity release curve of human triceps surae muscle. *J. Biomech.* **31**, 793-800.

Hof, A. L. (2003). Muscle mechanics and neuromuscular control. *J. Biomech.* **36**, 1031-1038.

Hof, A. L., van Zandwijk, J. P. and Bobbert, M. F. (2002). Mechanics of human triceps surae muscle in walking, running and jumping. *Acta Physiol. Scand.* **174**, 17-30.

Ker, R. F., Dimery, N. J. and Alexander, R. M. (1986). The role of tendon elasticity in a hopping wallaby (*Macropus rufogriseus*). *J. Zool. Lond.* **208**, 417-428.

Ker, R. F., Wang, X. T. and Pike, A. V. (2000). Fatigue quality of mammalian tendons. *J. Exp. Biol.* **203**, 1317-1327.

Komi, P. V. (1990). Relevance of in vivo force measurements to human biomechanics. *J. Biomech.* **23**, S23-S34.

Koob, T. J. and Summers, A. P. (2002). Tendon – bridging the gap. *Comp. Biochem. Physiol.* **133A**, 905-909.

Kubo, K., Kawakami, Y., Kanehisa, H. and Fukunaga, T. (2002). Measurement of viscoelastic properties of tendon structures in vivo. *Scand. J. Med. Sci. Sports* **12**, 3-8.

Lichtwark, G. A. and Wilson, A. M. (2005a). A modified Hill muscle model that predicts muscle power output and efficiency during sinusoidal length changes. *J. Exp. Biol.* **208**, 2831-2843.

Lichtwark, G. A. and Wilson, A. M. (2005b). Effects of series elasticity and activation conditions on muscle power output and efficiency. *J. Exp. Biol.* **208**, 2845-2853.

Lyman, J., Weinhold, P. S. and Almekinders, L. C. (2004). Strain behavior of the distal achilles tendon: implications for insertional achilles tendinopathy. *Am. J. Sports Med.* **32**, 457-461.

Maganaris, C. N. (2002). Tensile properties of in vivo human tendinous tissue. *J. Biomech.* **35**, 1019-1027.

Maganaris, C. N. and Paul, J. P. (2002). Tensile properties of the in vivo human gastrocnemius tendon. *J. Biomech.* **35**, 1639-1646.

Muramatsu, T., Muraoka, T., Takeshita, D., Kawakami, Y., Hirano, Y. and Fukunaga, T. (2001). Mechanical properties of tendon and aponeurosis of human gastrocnemius muscle in vivo. *J. Appl. Physiol.* **90**, 1671-1678.

Plagenhoef, S., Evans, F. G. and Abdelnour, T. (1983). Anatomical data for analysing human motion. *Res. Quart. Exercise Sport* **54**, 169-178.

Pollock, C. M. and Shadwick, R. E. (1994). Relationship between body mass and biomechanical properties of limb tendons in adult mammals. *Am. J. Physiol.* **266**, R1016-R1021.

Reeves, N. D., Narici, M. V. and Maganaris, C. N. (2003). Strength training alters the viscoelastic properties of tendons in elderly humans. *Muscle Nerve* **28**, 74-81.

Roberts, T. J. (2002). The integrated function of muscles and tendons during locomotion. *Comp. Biochem. Physiol.* **133A**, 1087-1099.

Roberts, T. J., Marsh, R. L., Weyand, P. G. and Taylor, C. R. (1997). Muscular force in running turkeys: the economy of minimizing work. *Science* **275**, 1113-1115.

Smith, C. W., Young, I. S. and Kearney, J. N. (1996). Mechanical properties of tendons: changes with sterilization and preservation. *J. Biomech. Eng.* **118**, 56-61.

Wang, X. T. and Ker, R. F. (1995). Creep rupture of wallaby tail tendons. *J. Exp. Biol.* **198**, 831-845.

Williams, P. L., Warwick, R., Dyson, M. and Bannister, L. H. (1989). *Gray's Anatomy*, 37th edn. London: Churchill Livingstone.

Wilson, A. M. and Goodship, A. E. (1994). Exercise-induced hyperthermia as a possible mechanism for tendon degeneration. *J. Biomech.* **27**, 899-905.

Zajac, F. E. (1989). Muscle and tendon: properties, models, scaling, and application to biomechanics and motor control. *Crit. Rev. Biomed. Eng.* **17**, 359-411.

Zuurbier, C. J., Everard, A. J., van der, W. P. and Huijing, P. A. (1994). Length-force characteristics of the aponeurosis in the passive and active muscle condition and in the isolated condition. *J. Biomech.* **27**, 445-453.